Методами фотометрії та електронної мікроскопії визначені функції розподілу частинок магнетиту, стабілізованих поверхнево-активною речовиною, за розмірами, і їх комплексний показник заломлення. За допомогою вимірювання коефіцієнта пропускання виконаний аналіз процесу седиментації наночастинок в ліпідо-магнетитових суспензіях різного складу і концентрації. За тимчасовим залежностям коефіцієнта пропускання розрахований ефективний середній радіус наночастинок. Ці частинки синтезовані як компонент біологічно-активних та харчових добавок

Ключеві слова: магнетит, фотометрія, електронна мікроскопія, розмір частинок, стійкість, ліпідо-магнетитова суспензія

Методами фотометрии и электронной микроскопии определены функции распределения частиц магнетита, стабилизированных поверхностно-активным веществом, по размерам, и их комплексный показатель преломления. С помощью измерения коэффициента пропускания выполнен анализ процесса седиментации наночастиц в липидо-магнетитовых суспензиях различного состава и концентрации. По временным зависимостям коэффициента пропускания рассчитан эффективный средний радиус наночастиц. Эти частицы синтезированы как компонент биологически-активных и пищевых добавок

Ключевые слова: магнетит, фотометрия, электронная микроскопия, размер частиц, устойчивость, липидо-магнетитовая суспензия

UDC 539.215.2:535.203.4
DOI: 10.15587/1729-4061.2016.76105

THE STUDY OF NANOPARTICLES OF MAGNITITE OF THE LIPID-MAGNETITE SUSPENSIONS BY METHODS OF PHOTOMETRY AND ELECTRONIC MICROSCOPY

A. Alexandrov
Candidate of Chemistry Sciences,
Associate Professor, Head of Department*
E-mail: alexandrov_a_v@inbox.ru
I. Tsykhanovska
Candidate of Chemistry Sciences,
Associate Professor*
E-mail: cikhanovskaja@rambler.ru
T. Gontar
Senior Lecturer*
E-mail: taty-gontar@mail.ru
N. Kokodiy
Doctor of Technical Sciences, Professor
Department of Theoretical Physics
Natsionalny Pharmaceutical University
Pushkinskaya str., 53, Kharkiv, Ukraine, 61002
E-mail: kokodiy.n.g@gmail.com
N. Dotsenko
PhD, Assistant
Department of mechanization and electrification of agricultural production
Mykolayiv State Agrarian University
Paris Commune str., 9, Nikolaev, Ukraine, 54010
E-mail: gorbenkonatalija@rambler.ru
*Department of Food and Chemical Technology
Ukrainian Engineering-Pedagogical Academy
Universitetskaya str., 16, Kharkiv, Ukraine, 61003

1. Introduction

At present, an important task facing food industry is expanding the range of products with improved nutritional value and long-term shelf life as well as saving scarce raw materials [1].

For normal functioning, a human organism must receive nutrients and energy in the amount adequate to the consumption. Lately, a lot of attention in nutrition is paid to lipids (animal fats and oils) – products with high nutritious and energy indices.

Nutritional properties (quality) of lipids are essentially influenced by their chemical transformations under the influence of temperature, water and other ingredients [2].

The presence of products of chemical and thermal transformations in lipids (fats, oils) significantly decreases their nutritional, energy and organoleptic indices and complicates their technological processing and assimilation [3, 4].

So, solution of the problem of chemical transformations (mostly oxidation) of lipids is very important – because these products are responsible for spoiling and reducing the shelf life of fats, oils and fat-containing food products and for decrease in their nutritional value and physiological safety [2–5].

Magnetite – double oxide of two- and trivalent iron ($FeO{\cdot}Fe_2O_3$) was studied as the antioxidant [6].

Given the positive influence of magnetite itself on a human organism [7] and the use of Fe_3O_4 as a source of assimilated iron [8], it is possible to use it in foods with the purpose

of enriching the body with Fe (II) and creation of the antianemic group of products (for treatment and prevention).

The entire set of the received data allows recommending Fe_3O_4 as a food supplement of the comprehensive action in lipid-magnetite suspensions (LMS), in which lipids form the dispersion medium (oils, melted animal fats, fat and oil composition) [4–6, 9].

Therefore, creation of the LMS which are stable in time, analysis of the process of their sedimentation, determining the size of the stabilized particles of magnetite Fe_3O_4, the functions of distribution by the size and their comprehensive index of refraction is a relevant and important task.

2. Literature review and problem statement

Because many of physical and chemical properties of nanoparticles, unlike voluminous materials, greatly depend on their size, the interest in the methods of measuring the nanoparticles dimensions in suspensions (solutions) has been considerably increasing lately; as a consequence, it is necessary to develop a set of methods of analysis for the measurement of parameters of nanoparticles.

In addition, to improve the quality indices of the products made of various materials (alloys, graphite products, plastics, pharmaceuticals, cosmetic products, food products, etc.) in the process of their obtaining, the use of nanopowders is becoming wider now. So, one of the promising directions of modern science is the development of nanotechnologies – the set of methods of obtaining and using nanoparticles [10].

Nanomaterials are divided into "nanostructured" materials and nanodispersions (nanosuspensions). Nanodispersions consist of dispersion medium (vacuum, gas, liquid or a solid body), in which nanoparticles, isolated from one another, are distributed [11]. The linear sizes of nanoparticles (from 1 to 100 nm) have one order of magnitude; normally, nanoparticles have the spheroid form. By virtue of their unique properties (for example, magnetic, bacteriostatic, germicidal, such as in magnetite) and their size, nanoparticles require careful studying. There are more than 20 ways of obtaining nanoparticles [11] and they can be conditionally divided into four groups:

– molecular clusters are obtained by chemical reactions in a solution or in gas phase;

– gas-phase clusters are obtained by condensation in the gas phase through initial vaporization;

– solid clusters appear as a result of solid-state chemical reactions or implanting ions;

– colloidal clusters are obtained by nucleation from solutions and melts or through the sol-gel transformations.

The processes, as a result of which nanostructures are formed, include crystallization, re-crystallization, phase transformations, high mechanical loads and intensive plastic deformation, full or partial crystallization of amorphous structures [10, 11]. The characteristics of the obtained product – granulometric composition and the shape of particles, the content of impurities and the magnitude of specific surface can vary in a fairly wide range depending on the method of obtaining.

The industries of different countries use a variety of nanoparticles of different chemical composition, but their application does not always yield desirable results, which is mostly due to the unawareness of their true size, defining which is a fairly complicated problem. So, for example, the use of the same nanoparticles that are different in size (because of various production technologies or application of different methods of defining their size), leads to obtaining finished products with different properties.

Next, we will list the most common methods of defining the size of nanoparticles [10–28]:

– electronic microscopy (based on the analysis of the sample using a beam of accelerated electrons) [10–16];

– transilluminating electronic microscopy (transillumination of the sample with a beam of electrons with determining the size and internal structure of the particles) [10, 11];

– scanning (raster) electronic microscopy (scanning the sample surface with a beam of electrons with simultaneous registration of secondary electrons and obtaining a 3-D image) [10, 12];

– scanning probe microscopy (analysis of relief of the sample surface with the use of a probe) [10, 13];

– scanning tunnel microscopy (analysis of relief of the current-conducting surfaces by registering the magnitude of tunnel current that occurs between the tip of the probe and the surface of the sample) [10, 14];

– atomic-power microscopy (analysis of relief and mechanical properties of the surfaces by registering the magnitude of van der Waals forces occurring between the tip of the probe and the surface of the sample) [10, 15];

– light scattering (the method of statistical dispersion of light) (determining the size of the particles by the intensity of scattered light) [10, 16];

– photon correlation (the method of dynamic dispersion of light) (determining the size of the particles by the coefficient of diffusion that is defined by the intensity and frequency characteristics of scattered light) [10, 16];

– small-angular scattering (X-rays and neutrons) (assessment of the size of the particles by the angular dependence of intensity of diffuse scattering (in the field of small angles)) [10, 17];

– diffraction methods (X-ray diffractometry – electronic – neurography) (diffraction of radiation on the crystal lattice of the sample with obtaining diffractogram and estimation of the size of crystals by the magnitude of expansion of diffraction maxima) [10–18];

– sedimentation (determining the size of the particles by the rate of their sedimentation); adsorption method (BET – theory of Brunauer, Emmet and Teller) (determining the specific surface (the size of the particles) of the sample by measuring the magnitude of the low-temperature adsorption of inert gases (nitrogen)) [10, 18].

The researchers measured the size of the particles of iron by various methods. Table 1 shows to what extent the obtained results may vary [10].

Table 1

Results of determining the size of Fe particles, obtained by different methods

Method of analysis	Size of particles, nm
Scanning electronic microscopy	50–80
Transilluminating electronic microscopy	300–1000
X-ray diffractometry	20
Small-angular diffraction: neurography	24–64
Low-temperature adsorption (BET)	60
Static light scattering	50–8000
Dynamic light scattering	70

The generally accepted way of determining the size of nanoparticles is their studying using transilluminating electronic microscopes. But, for example, titanium nitride, TiN, produced by NaBond Technologies Co, Ltd, HONG KONG [12], is impossible to categorize based on its results, although the size of its particles does not exceed 100 nm. Besides, the nanoparticles are prone to formation of conglomerates. These data are presented in the works [13, 14]. A comprehensive idea of the disparsity of powder is given by knowing the totality of such characteristics as the size of the particles, their total specific surface and morphology. There are many methods of determining the size of the particles, which use different physical principles such as laser diffraction of light stream on the particles, sedimentation of the particles by weight in dispersion medium.

A significant contribution to studying the size, geometry and morphology of particles is made by the method of determining their specific surface as well as scanning electronic microscopy [10, 15, 16]. In this case, though not always equal by the principles of research, the methods give similar results, which was shown in the paper [15] when assessing the ultrathin tungsten powder by the methods mentioned above.

The difficulty of determining the size of the powder particles lies in the fact that they are prone to agglomeration [10, 15].

Other methods for determining the size of the nanopowder particles are also used, but, as their analysis showed, none of them gives the exact size of nanoparticles [10]. So, in the papers [17], the kinetics of sedimentation processes and the stability of suspensions with supermagnetic nanoparticles of ferrum oxide were analyzed by the methods of sedimentation and nuclear magnetic resonance (NMR). The disadvantage of this method is inaccuracy (in case of sedimentation) and the use of expensive equipment (NMR). Lack of accuracy is observed in determining the stability of magnetite suspension in the complex method (viscosimetry+sedimentation) [18]. In the fluorescent method, there are some restrictions due to the limited capabilities of standard fluorescent devices. The disadvantage of the laser methods [19] is dependence of the measurement results on the condition of the surface of the particles in suspension. The differential capacity of the system differential motion analyzer (DMA) [20, 21] and the accuracy of measurement vary depending on temperature and pressure. The disadvantages of the optical method of "measuring indicatrix of the scattered particles of light" [22–24] are the complexity of measurement of the form of indicatrix of scattering and the necessity to know the refraction index. Besides, the method cannot be applied to measure the size of the nanoparticles because the width of the first petal of indicatrix becomes very large, larger than 90°, and the accuracy of measurement is significantly reduced. The disadvantages of the method of "dynamic scattering of light" [25] is the complexity of experimental equipment that should give the possibility to measure very small intensities of scattered light and the inability to measure the size of the microparticles. In the article [26], the methods of spectrophotometry and scanning electronic microscopy were proposed for studying the extaction and morphological characteristics of magnetite particles in aqueous suspensions. The disadvantage is the fact that these methods are unacceptable for lipid suspensions. In the optic method of determining the concentration and size of the particles of magnetite by using the fluctuations of transparency, the research is based on the hydrogen suspensions of magnetite, which is why it is not suitable for lipid-magnetite suspensions [27]. With the spectrophotometric [28] method, it is difficult to process the data, although the method has high accuracy.

That is why, researchers of the sizes and morphological characteristics of nanoparticles who have been working with ultra-thin particles for years, state "for an objective evaluation of the properties and the morphology of nanopowders, development of the set of methods of analysis is necessary".

Besides, in the literary sources [10–28] we have not found any facts of using the methods of photometry and electronic microscopy for studying morphological characteristics and optical properties of magnetite nanoparticles in LMS, based on the processing attenuation spectrum and e-microphotography of Fe_3O_4 nanoparticles (histogram): of the sizes, of the functions of distribution of Fe_3O_4 particles by size and of their comprehensive index of refraction.

Therefore, using the methods of photometry and electronic microscopy, the process of sedimentation of LMS of different composition and concentrations was studied; the sizes of the stabilized particles of magnetite Fe_3O_4, the functions of distribution by size and their comprehensive index of refraction were defined.

3. The aim and the tasks of the study

The aim of the work is to study the process of sedimentation of lipid-magnetite suspensions of different composition and concentration by the methods of photometry and electronic microscopy, to determine the size of the stabilized particles of magnetite Fe_3O_4, the functions of distribution by size and their comprehensive index of refraction.

To achieve the goal, the following tasks were set:

– analysis of dependence of the light transmission factor by lipid-magnetite suspension (LMS) on the wavelength and the time of exposure of the LMS at different wavelengths of light and assessment of the suspension stability over time;

– determining the size of the magnetite particles, stabilized by the surface active substance (monoacylglycerol), using the methods of electronic microscopy and photometry as well as distribution of particles by size f(r), their indices of refraction (n) and absorption (k), the concentration N; analysis of changes in the concentration of magnetite particles in the LMS in time;

– determining and analysis of the spectra of transmission of the diluted LMS of different composition and concentration;

– determining the kinetic dependency of the transmission factor for the suspensions with different concentration of magnetite and the mean effective radius of the particles.

4. Materials and methods of studying sedimentation resistance of lipid-magnetite suspensions

4. 1. Studied substances and equipment used in the experiment

While obtaining the suspensions, ultra-thin magnetite (with the particle size of 30–60 nm) was used, which was synthesized according to the well-known method of co-sedimentation of salts of two- and trivalent ferrum in alkaline medium [29].

In the study we used the sunflower refined deodorized oil in accordance with DSTU 4492:2005; non-refined corn

oil DSTU GOST 8808-2003 "Corn oil. Technical specifications (GOST 8808-2000. IDT)"; non-refined soybean oil DSTU 4534:2006 "Soybean oil. Technical conditions"; pork fat in accordance with GOST 25292-82; beef fat GOST 1288-41; salomas unrefined for margarine industry TU 9145-181-00334534-96, TU 15.4-13304871-005:2005; substitute of milk fat "Violia-milk fat 3" TU15.4-13304871-005:2005, GOST P 53796-2010; confectionery fat «Shortening» TU U-15.4-00373758:022-2006; PAR (monoacylglycerol) Dimodan HP.

In Fig. 1, the following lipids are presented: oils (soybean, corn, sunflower); salomas, beef, pork and confectionery fats "Violia-milk fat 3" and "Shortening".

Fig. 1. The studied lipids

Lipid-magnetite suspensions (LMS) were received by the technology [7]. The LMS with magnetite, obtained by this way, as a dispersion phase, have vegetable or animal fats as dispersion medium.

The study of stability and concentration of the suspensions, morphological features of the particles was carried out using spectrophotometry (spectrometer Specol 11) or PE-5400 UV (TOV "Ecochim") and eletronic microscopy (transmission electronic microscope (TEM) JSM-820 (JEOL).

4. 2. Methods of determining stability, dispersity of lipid-magnetite suspensions of different composition, concentration, as well as the sizes, functions of distribution of Fe_3O_4 particles by size and their comprehensive index of refraction

The method is based on the analysis of attenuation spectrum of suspension with the nanoparticles. It is possible to get acquainted with the method of determining the stability, dispersity of lipid-magnetite suspensions of different composition, concentration, as well as the size, function of distribution of Fe_3O_4 particles by size and their comprehensive index of refraction in the paper [30–35].

5. Results of studying sedimentation and aggregation stability of morphological characteristics of LMS

The results of measurement of the transmission factor (T, %) depending on the wavelength of light (λ, nm) over time (the ratio Fe_3O_4:SAS= =0,05:0,70 mass %; the concentration of suspension 29,25 mg/l) are shown in Table 1 and in Fig. 2, 3.

Table 1

Results of measurement of the transmission factor (T, %) depending on the wavelength of light (λ, nm) over time for the soy-magnetite suspension

λ, nm	Transmission factor T, %					ΔT, %
	Exposure time of suspension τ, hours					
	0	0,5	1,0	24,0	48,0	
210	25	25,6	26,3	26,9	27,5	10,0
250	23	24,1	25,2	26,7	27,2	18,3
300	26	26,5	27,3	28,5	29,9	15,0
350	28,2	29,7	31,4	32,9	34,4	21,9
400	29	30,6	31,9	33,8	35,7	23,1
450	33,1	34,4	35,7	37,3	39,5	19,3
500	31,5	33,8	34,5	35,6	38	20,6
550	30,5	32,6	33,3	34,5	36,8	20,6
600	48,6	50,7	52,8	58,2	63,5	30,7
650	54,6	55,8	58,4	63,5	68,7	25,8
700	57,8	59,6	62,5	66,7	71,3	23,4
750	58,5	60,3	64,6	68,3	72	23,1
800	61,2	62,9	66,5	70,3	74,6	21,9
850	64,5	66,2	68,6	72,5	76,1	18,0
900	69,6	70,9	73,4	76,3	80	14,9
950	71,6	72,3	73,9	76,9	80,9	13,0
1000	71,9	72,5	73,7	77	81, 2	12,9

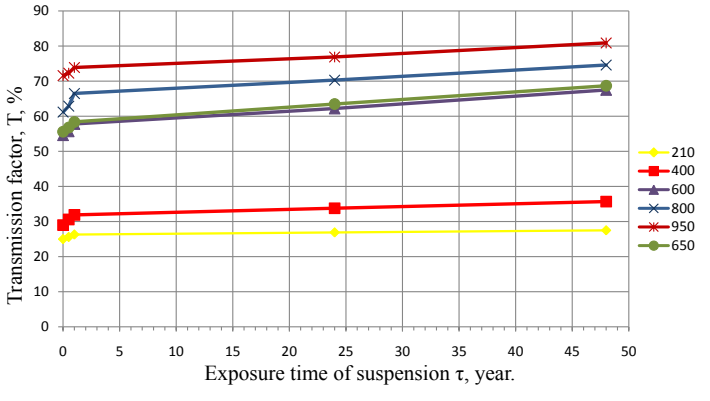

Fig. 2. Dependence of the transmission factor (T, %) on the wavelength of light λ (nm) over time for the soy-magnetite suspension (SMS)

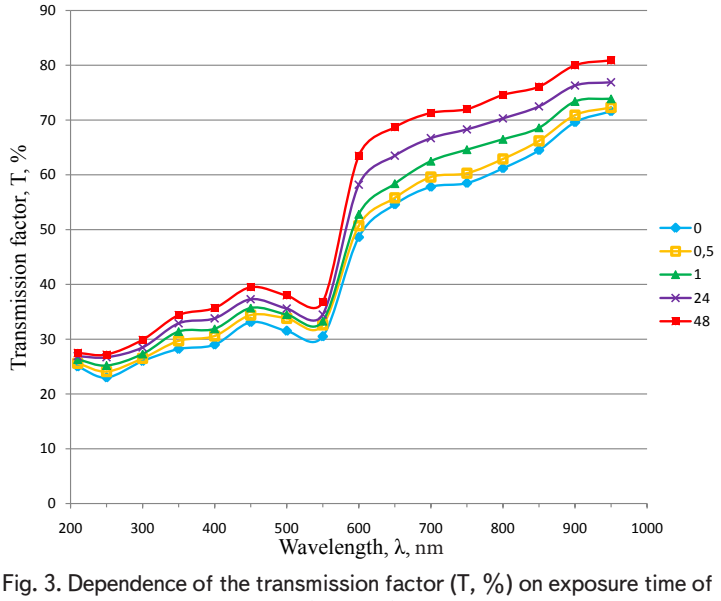

Fig. 3. Dependence of the transmission factor (T, %) on exposure time of the soy-magnetite suspension (τ, hours) at the different wavelengths of light (λ – from 210 to 1000 nm)

A typical view of experimental dependence $\alpha(\lambda)$ for the soy-magnetite suspension is presented in Table 2 and in Fig. 4. In this case, α_i and λ_i were determined by formulas (11), (12) n_0=1,48 – index of refraction of dispersion medium (soybean oil), determined experimentally.

Table 2

Results of calculation of λ_i and α_i of the suspension

λ_0(nm) – T_i (%); T_i (u. sh.)	λ_i, μm	ln T_i	α_i, m^{-1}
210 – 25,0; 0,25	0,142	1,65	165
250 – 23,0; 0,23	0,169	1,47	147
300 – 26,0; 0,26	0,203	1,31	131
350 – 28,2; 0,282	0,236	1,18	118
400 – 29,0; 0,29	0,27	1,045	104,5
450 – 33,1; 0,331	0,304	0,93	93
500 – 31,5; 0,315	0,34	0,82	82
550 – 30,5; 0,305	0,374	0,72	72
600 – 48,6; 0,486	0,408	0,66	66
650 – 54,6: 0,546	0,142	0,61	61
700 – 57,8; 0,578	0,169	0,57	57
750 – 58,5; 0,585	0,203	0,536	53,6
800 – 61,2; 0,612	0,236	0,5	50
850 – 64,5; 0,645	0,27	0,465	46,5
900 – 69,6; 0,696	0,304	0,442	44,2
950 – 71,6; 0,716	0,34	0,414	41,4
1000 – 71,9; 0,719	0,374	0,395	39,5

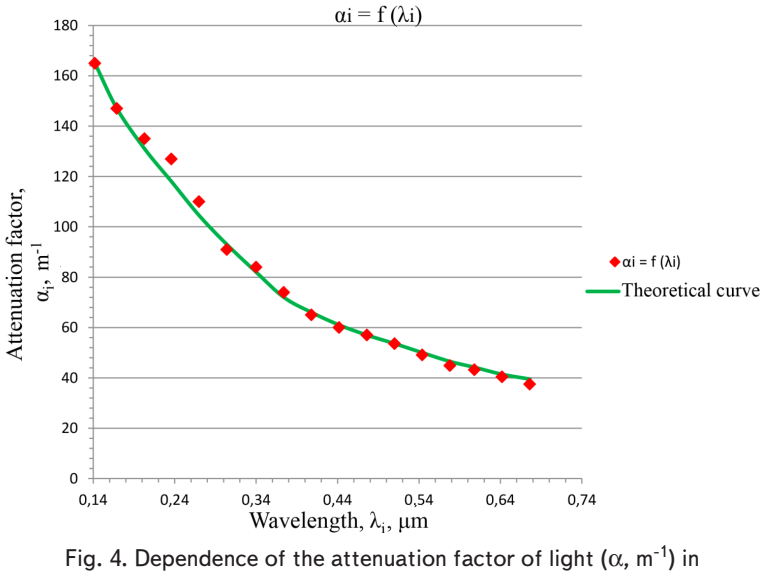

Fig. 4. Dependence of the attenuation factor of light (α, m^{-1}) in the soy-magnetite suspension on the wavelength (λ, μm)

The theoretical curve was built up by approximation of experimental data of the dependence of attenuation factor on the wavelength.

Using the equation:

$$\alpha(N, r, m, \lambda) = N\pi r^2 Q(r, m, \lambda),$$

where r is the radius of the particle, m=n–iκ, n is the index of refraction, k is the absorption index, λ is the wavelength in the medium that surrounds the particle, Q is the factor of attenuation efficiency.

Mean radius of the particles r and the parameters n, κ, and N were determined. For this purpose, the function was built:

$$S(r, n, \kappa, N) = \sum_{i=0}^{i_{max}} \left[N\pi r^2 Q(r, n, \kappa, \lambda_i) - \alpha_i \right]^2,$$

where λ_i is the wavelength, at which the attenuation factor α_i was measured.

The values of parameters r, n, κ, N, at which function S (r, n, κ, N) has a minimum, were determined by the method of the least squares. The calculation of minimization function was performed using the Mathcad software program.

An additional control of the views of graphs with the experimental points α_i and curve α (r, n, N, κ, λ), which must pass near these points, was carried out (Fig. 4). The value of function S (r, n, κ, N), which also depends on the initial approximations and must be minimal, was controlled.

For the studied soy-magnetite suspension, the following values were obtained r=38 nm, n=1,48, κ=0,01, N=1,43×$\times 10^{12}$ m^{-3}.

The values of indices of refraction and absorption correlate satisfactorily with the reference data for magnetite: in the range of wavelengths from 0,4 to 0,8 μm, its refraction index changes from 1,9 to 1,7, and the rate of absorption – from 0,1 to 0,01.

The obtained data were used in the MathCAD program for determining the parameters β and μ in the function of distribution of particles by size.

Fig. 5 shows the graph of normed function of distribution of particles f(r) by size.

For comparison, Fig. 6 shows the histogram of distribution of the particles of magnetite in the soy-magnetite suspension (SMS) by size, obtained as a result of processing the observations with the use of the electronic microscope, which shows that the results of both methods are consistent with one another.

Fig. 7 shows the image of the particles made in the course of electronic and microscopic observations.

As one can see in the given transmission microscope – TMM (Fig. 7), aggregation of the particles occurs with formation of clusters. Grouping of the particles in clusters provides the circuit of magnetic flux and can be explained by the absence of external magnetic field when conducting the electronic and microscopic studies [35]. In this case, it can be clearly seen that the clusters consist of small particles; the boundaries of each particle are clearly visible.

Knowing the size of the particles, their concentration in the suspension was also found. Table 3 and Fig. 8 display results of the study of changes in the quantity (concentration) of particles per 1 cm^3 of the suspension during 45 days.

Table 3

Quantity of particles per 1 cm^3 of the soy-magnetite suspension

Quantity of magnetite particles per 1cm^3 of suspension	Exposure time of SMS, τ, h					
	0	0,5	1,0	24,0	48,0	1080,0
	$1,43 \cdot 10^{12}$	$1,42 \cdot 10^{12}$	$1,40 \cdot 10^{12}$	$1,34 \cdot 10^{12}$	$1,23 \cdot 10^{12}$	$1.19 \cdot 10^{12}$

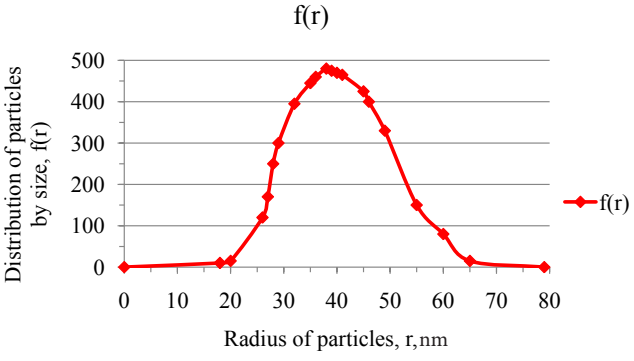

Fig. 5. Distribution of particles of magnetite in the soy-magnetite suspension (SMS) by size, measured by optical method

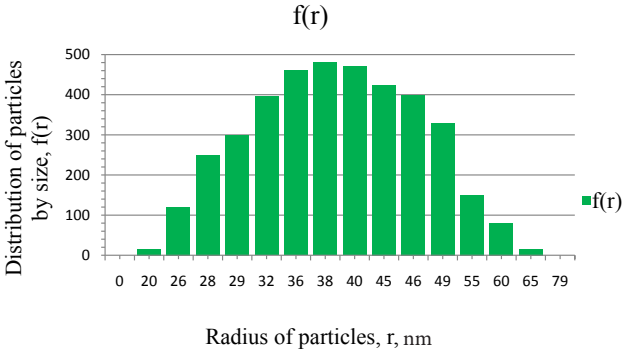

Fig. 6. Histogram of distribution of the particles of magnetite in the soy-magnetite suspension (SMS), obtained as a result of processing observations using the electronic microscope

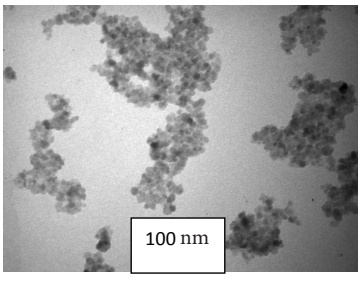

Fig. 7. Electronic microphotograph of the particles of magnetite in SMS

By the experimental data, given in Table 3 and in Fig. 8, it is possible to tell sedimentation stability and dispersity of LMS (by the example of SMS).

The experimental data on the dependence of transmission factor (T, %) on the wavelength of light (λ, nm) for the soy-magnetite suspensions (SMS) of different composition and with different concentration of $Fe_{(tot.)}$ are shown in Tables 4, 5 and Fig. 9, 10.

Transmission spectra of diluted suspensions (concentration of 4,85 mg/l) are shown in Fig. 9.

The assessment of the aggregation stability was carried out using the kinetic measurements.

Fig. 10 shows kinetic dependences of the transmission factor for suspensions with different concentration of magnetite (Fe_{tot}) and the SMS without stabilizer (monoacylglycerol). The efficiency of the applied method of stabilization may be evaluated by comparing the kinetics of sedimentation to the case of the soy-magnetite suspension of equal concentration, in which there was no a surface active substance (stabilizer). Existence of different fractions of magnetite particles and the intensity of their aggregation determines the non-linear law of change in the transmission coefficient for magnetite suspensions without a stabilizer or with high content of magnetite.

Approximating the obtained dependences by straight lines and extrapolating them to achieving T=100 %, it is possible to estimate the average effective radius of the particles. Table 6 and Fig. 11 present the temporary dependences of the transmission factor of the studied suspensions at the wavelength of 600 nm. The obtained values of sedimentation time and effective mean radius are given in Table 7.

By the data of Table 7, it is possible to estimate the effective radius of particles in the LMS of different concentration as well as the aggregation stability of suspensions.

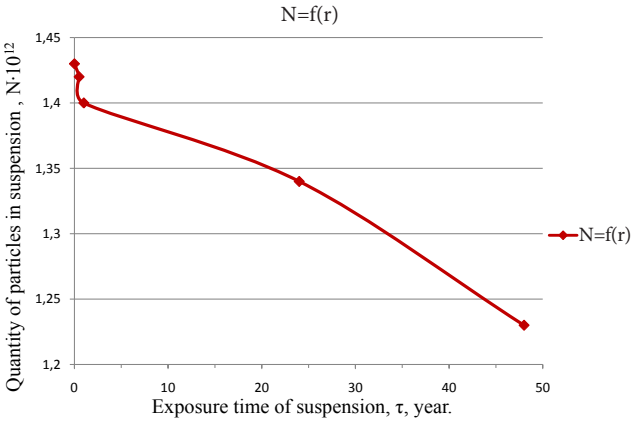

Fig. 8. Change of concentration of magnetite particles in the soy-magnetite suspension over time

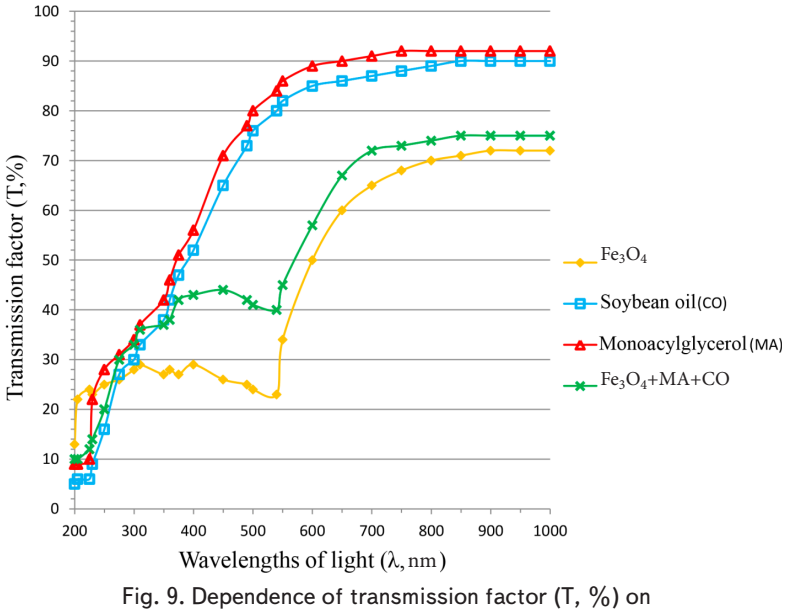

Fig. 9. Dependence of transmission factor (T, %) on the wavelength of light (λ, nm) for the soy-magnetite suspensions (SMS) of different composition

Table 4

Dependence of transmission factor (T, %) on the wavelength of light (λ, nm) for the soy-magnetite suspensions (SMS) of different composition (the concentration of suspensions is 4,85 mg/l)

Wavelength of light (λ, nm)	Fe_3O_4	Monoacylglycerol	Soy bean oil (SO)	Fe_3O_4+MA	Fe_3O_4+CO	MA+CO	Fe_3O_4+MA+CO
200	13	9	5	9	7	10	10
205	22	9	6	11	9	12	10
225	24	10	6	14	13	16	12
230	23	22	9	20	18	19	14
250	25	28	16	26	23	25	20
275	26	31	27	29	27	28	30
300	28	34	30	35	31	32	33
310	29	37	33	39	35	36	36
350	27	42	38	43	39	39	37
360	28	46	42	40	36	44	38
375	27	51	47	44	40	48	42
400	29	56	52	50	48	52	43
450	26	71	65	47	46	54	44
490	25	77	73	43	44	62	42
500	24	80	76	42	43	66	41
540	23	84	80	41	42	71	40
550	34	86	82	47	49	78	45
600	50	89	85	56	58	82	57
650	60	90	86	64	66	85	67
700	65	91	87	72	70	87	72
750	68	92	88	78	76	90	73
800	70	92	89	82	80	92	74
850	71	92	90	82	80	92	75
900	72	92	90	81	79	92	75
950	72	92	90	80	79	91	75
1000	72	92	90	80	79	91	75

Table 5

Dependence of transmission factor (T, %) on the wavelength of light (λ, nm) for the soy-magnetite suspensions (SMS) of different concentration

Wavelength of light λ, nm	Transmission factor T, %			
	Concentration of $Fe_{tot.}$ in suspension, mg/l			
	4, 85 mg/l	9,75 mg/l	19,5 mg/l	38,9 mg/l
200	25	16	12	10
205	26	17	13	10
225	28	19	15	12
230	31	24	17	14
250	33	28	19	16
275	35	30	21	19
300	37	32	24	21
310	40	36	27	24
350	43	39	30	27
360	46	42	33	30
375	48	45	36	33
400	52	49	39	36
450	53	50	40	37
490	50	48	38	35
500	46	45	37	33
540	45	44	36	32
550	48	46	37	35
600	57	55	48	47
650	67	63	59	53
700	76	72	64	56
750	81	75	69	59
800	84	77	73	65
850	86	79	75	68
900	86	80	77	68
950	86	80	77	68
1000	86	80	77	68

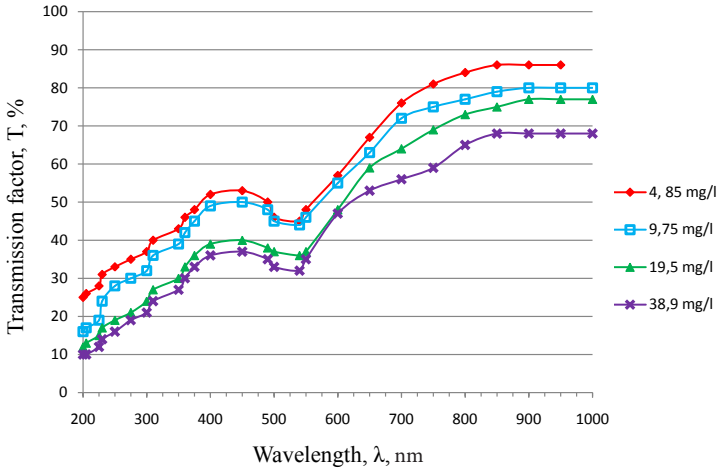

Fig. 10. Dependence of transmission factor (T, %) on the wavelength of light (λ, m) for the soy-magnetite suspensions (SMS) of different concentrations

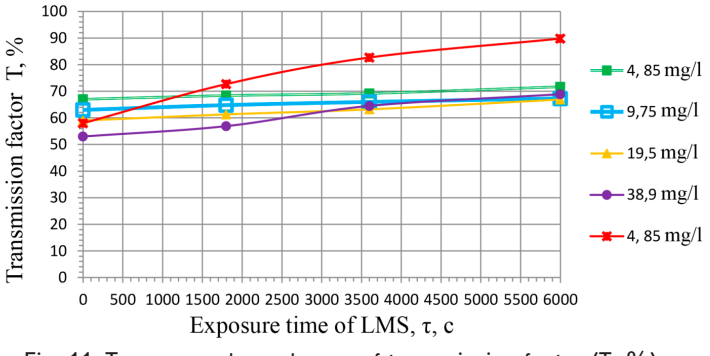

Fig. 11. Temporary dependences of transmission factor (T, %) on the wavelength of 600 nm for the soy-magnetite suspensions (SMS) of different concentrations

Table 6

Temporary dependences of transmission factor (T, %) of the soy-magnetite suspensions (SMS) of different concentrations on the wavelength of light (λ=600 nm)

Transmission factor T, %					
Exposure time of suspension τ, h.	Concentration of Fe_{tot} in suspension, mg/l				
	4,85 mg/l	9,75 mg/l	19,5 mg/l	38,9 mg/l	4,85 mg/l without SAS
0	67	63	59	53	58
1800	68,4	64,8	61,3	56,9	72,7
3600	69,2	66	63,2	64,5	82,7
6000	71,7	67,3	66,9	68,9	89,8

Table 7

Results of calculation of sedimentation time t_{sed} and mean effective radius of the particles r_{eff} at different concentration of suspension

Parameter	Concentration of $Fe_{tot.}$, mg/l			
	4,85	9,75	19,5	38,9
t_{sed}, time	454	228	168	147
r_{eff}, nm	76	92	146	168

6. Discussion of results of studying stability of LMS

Synthetic magnetite (Fe_3O_4) is ultra-thin black powder, the size of the particles is of the order 30 nm, non-toxic, possesses useful properties: bactericidal, bacteriostatic, demonstrates antioxidant activeness; has beneficial effect on a human organism; is a source of easily assimilated iron [6–9]. That is why Fe_3O_4 may be proposed as a dispersion phase in the lipid constituents of biologically active and food supplements.

The obtained various lipid-magnetite suspensions, in which refined deodorized sunflower oil, unrefined corn oil, unrefined soybean oil, beef fat, pork fat, unrefined salomas for margarine industry, milk fat substitute "Violia-Molfat 3" and confectionary fat "Shortening" were used as dispersion medium.

Using the methods of photometry and electronic microscopy, the assessment of sedimentary stability of the lipid-magnetite suspensions was carried out, the sizes of particles of magnetite with SAS, the functions of distribution of the particles of magnetite Fe_3O_4 by size were determined, their comprehensive index of refraction and their concentration in suspensions, for example, the diameter of the particles in the soy-magnetite suspension equals 76 nm.

Analysis of Fig. 2 and Table 1 shows that in the course of time (0–48,0 hours) and with an increase in the wavelength (210–1000 nm), we observed a gradual increase in the transmission factor from 25 % (210 nm) to 71,9 % (1000 nm) at 0 hours of suspension exposure; from 27,5 % (210 nm) to 81,2 % (1000 nm) at the maximum exposure time of suspension (48 hours).

From Table 1 and Fig. 3 it is also visible that the largest change in the transmission factor (ΔT, %) with the course of time is observed at wavelengths 600 and 650 nm (30,7 and 25,8 %), respectively. At other wavelengths, ΔT was equal to approximately 18,4 %. Therefore, taking into account the accuracy of the photometric diagnostic method for determining stability of the suspension, it is better to recommend the wavelengths at which the accuracy of determining will be higher, i. e., 600–650 nm; then ΔT starts to fall gradually. The kinetic studies were also carried out at the wavelength of light of 600 nm.

It was experimentally found that all studied lipid–magnetite suspensions are rather stable over time. Various ratios of components of the lipid-magnetite suspensions were studied, in this case, the best results of stability were demonstrated by the suspensions in which the ratio of Fe_3O_4:SAS=0,02 g:0,35 g or 0, 04 of mass %:0,70 mass % and 0,025 %:0,35 g or 0,05 mass %:0,70 mass %. Since the study relied on the medical and biological requirements, the suspensions with the ratio of Fe_3O_4:SAS=0,025 g:0,35 g or 0,05 mass %:0,70 mas % were selected.

Based on the analysis of the experimental points $\alpha_i=f(\lambda_i)$ (Table 2) and the theoretical curve $\alpha=f(r, n, N, \kappa, \lambda)$, which was built up by approximation of the experimental data of the dependence of attenuation factor on the length of wave which passes near these points (Fig. 4), the following values for the soy-magnetite suspension (SMS) were obtained: r=38 nm,

n=1.48, κ=0.01, N=1,43×10^{12} m^{-3}. In this case, the value of function S (r, n, κ, N), which also depends on the initial approximations and should be minimal, was also controlled.

It should be noted that the values of the indices of refraction (n) and absorption (κ) correlate satisfactorily with the reference data for magnetite; in the range of wavelengths from 0,4 to 0,9 μm the index of refraction changes from 1,9 to 1,7, and the absorption index – from 0,1 to 0,01.

The obtained results were used in the MathCAD program to calculate minimization function and to determine parameters β and μ in the function of distribution of particles by diameter. Fig. 5 shows the graph of the normed function of particles distribution f(r) by size that correlates well with the histogram (Fig. 6), received as a result of processing the TMM data of the SMS sample images (Fig. 7). The number of particles in the sample for determining the average values was not less than 500. The established function is symmetric and rather narrow, which indicates the system of the synthesized nanoparticles as homogeneous with a low degree of polydispersity. The established order of the average size of the particles is <d>~38 nm.

The concentration (the number of particles in 1 cm^3) of suspension was determined, which, for example during preparation, is N=1,43·10^{12} cm^{-3}.

The decrease in the number of particles of magnetite with SAS in 1 cm^3 of the soy-magnetite suspension was established: within 48 hours, the concentration in 1 cm^3 decreased by 20 % – from 1,43·10^{12} to 1,19·10^{12} cm^{-3} (Table 3).

Analysis of Table 3 and Fig. 8 demonstrates that the number of particles in a layer of suspension decreases by 0,7 % within 0,5 hours, within 1,0 hour – by 2,1 %; within 24 hours – by 6,7 %, within 48 hours – by 16,5 % and in 45 days – by 20.0 %. The obtained data indicate partial homogeneity of the particles of magnetite – the largest particles settle within the first 24 hours.

The analysis of the sedimentation process in suspensions of different composition and concentration was carried out by measuring the transmission factor.

The optical transmission spectra were studied for the soy-magnetite suspensions (SMS) of different concentrations.

To determine the contribution of individual components of the solution to the resulting spectrum, the suspensions of magnetite without a stabilizer were prepared. The obtained optical transmission spectra are given in Tables 4, 5 and in Fig. 9, 10. In UV-Spectra (Fig. 9), there are weak transition strips n→π* at 200–210 nm, which are characteristic for the saturated acyl radicals (monoacylglycerol – MA), and the stronger transition strips π→π* at 210–230 nm, which are characteristic for the α, β-unsaturated acyls (soybean oil – SO). In the spectrum of magnetite, broad absorption strips are observed in the area of 490 and 540 nm, associated with lattice fluctuations of Fe–O – links in tetra- and octahedral positions of Fe_3O_4. By comparing these curves of dependence of the transmission factor on the wavelength for the SMS, the special features of the spectrum, characteristic for magnetite, monoacylglycerol and soybean oil, can be seen.

The comparison of the transmission spectra of suspensions with different degrees of dilution (Fig. 10) shows chemical identity of the samples. The evaluation of aggregate stability was carried out using the kinetic measurements. In Table 6 and Fig. 11, the dependence of kinetic transmission factor for suspensions with different concentration of magnetite (Fe_{tot}) and the SMS without a stabilizer (monoacylglycerol) is shown. Analysis of Fig. 11 shows a nonlinear law of changing the transmission factor for magnetite suspensions without a stabilizer or with high content of magnetite (38,9 mg/l), which can be explained by existence of different fractions of the particles of magnetite and their aggregation. In the UV-area of the spectrum, at low concentrations there is a direct proportionality between the transmission factor and the concentration of ($Fe_{заг.}$), i. e., absorbing centers of Fe_3O_4.

The calculation of the effective mean radius (Table 7) for SMS with the concentration of 38,9 mg/l gives a lowered value, which, probably, is predetermined by the constraints of linear approximation, as the dependence T(t) in this case is nonlinear. One can make an assumption that an increase in the concentration to 38,9 mg/l results in significant decrease in the aggregation stability.

The average radius of the particles of magnetite in the lipid suspension without a stabilizer is possible to be estimated reliably in this way, the linear extrapolation of the curve allows receiving (r_{eff})=400 nm. Visually, the SMS demonstrated high aggregation stability with the total sedimentation time equal to several tens of hours.

The estimation of the effective mean radius of the particles from the kinetics of sedimentation gives the value of 76–168 nm, and the dependence (r_{eff}) on C(Fe(ov.)) has a linear character up to the concentration of 38.9 mg/l. The process of sedimentation in the case of high concentrations and pure magnetite, which is not stabilized by monoacylglycerol, has a distinctly expressed nonlinear character, which is connected with the intensive aggregation of the particles and different sedimentation rate for various fractions.

7. Conclusions

1. We conducted evaluation of sedimentation and aggregate stability of the lipid-magnetite suspensions (in which the dispersion medium was created by corn, sunflower, soybean oil, beef and pork fats, confectionery fats, salomas). All suspensions are stable enough over time. The best results for stability were demonstrated by suspensions, in which the ratio Fe_3O_4:SAS=0,02 g:0,35 g or 0,04 mass %:0,70 mass % and 0,025:0,35g or 0,05 mass %:0,70 mass %. The size of the particles of magnetite with SAS was determined. Diameter of the particles is 76 nm. It was found that over time (0–48.0 h) and with increasing the length of the wave (210–1000 nm), a gradual increase in the coefficient of transmission is observed, from 25 % (210 nm) to 71.9 % (1000 nm) at 0 hours of suspension exposure; from 27.5 % (210 nm) to 81.2 % (1000 nm) at the maximum exposure time of suspension (48 hours).

2. We determined concentration of the particles of magnetite, stabilized by a surface active substance – the concentration (the number of particles in 1 cm^3) during preparation of suspension is equal to N=1,43·1012 cm^{-3}. The reduction in the number of particles of magnetite with SAS per 1 cm^3 of the soy-magnetite suspension was revealed: in 48 hours, the concentration per 1 cm^3 decreased by 20 % – from 1,43·10^{12} to 1,19·10^{12} cm^{-3}. The following values for the soy-magnetite suspension (SMS) were defined: r=38 nm, n=1,48, κ=0,01. The established distribution function is symmetric and rather narrow, which indicates that the system of the synthesized nanoparticles is homogeneous with a low degree of polydispersity. The defined order of the average size of the particles is <r>~38 nm.

3. In the UV-Spectra, there are weak transition strips $n \rightarrow \pi^*$ at 200–210 nm, which are characteristic for the saturated acyl radicals (monoacylglycerol – MA) and the stronger transition strips $\pi \rightarrow \pi^*$ at 210–230 nm, which are characteristic for the α, β-unsaturated acyls (soybean oil – SB). In the spectrum of magnetite, broad strips of absorption are observed in the area of 490 and 540 nm, associated with lattice fluctuations of the Fe-O-links in tetra- and octahedral positions of Fe_3O_4. By comparing these curves of dependence of the transmission factor on the wavelength for SMS, the special features of the spectrum, characteristic for magnetite, monoacylglycerol and oil (lipid), can be seen. A comparison of the transmission spectra of suspensions with different degrees of dilution shows chemical identity of the samples.

4. Analysis of the kinetic dependencies of coefficient of transmission for LMS shows a nonlinear law of change in the coefficient of transmission for suspensions without a stabilizer or with high content of magnetite (38.9 mg/l), which can be explained by existence of different fractions of the particles of magnetite and their aggragation. In the UV area of the spectrum, at low concentrations, there is direct proportionality between the transmission coefficient and the concentration $Fe_{(ov.)}$, i. e., absorbing centers of Fe_3O_4. The estimate of effective mean radius of the particles from the kinetics of sedimentation gives value of 76–168 nm, in this case, up to the concentration of 38.9 mg/l, the dependence (r_{eff}) on $C(Fe_{(ov.)})$ has linear character. The process of sedimentation in the case of high concentrations and pure magnetite, which is not stabilized by monoacylglycerol, displays vividly expressed nonlinear character associated with intensive aggregation of the particles and different rates of sedimentation for various fractions.

References

1. Skurihin, I. M. VsYo o pische s tochki zreniya himika [Text] / I. M. Skurihin. – Moscow: Vyissh.shk., 1991. – P. 33–40.
2. Tyutyunnikov, B. N. Himiya zhirov; 3rd edition [Text] / B. N. Tyutyunnikov. – Moscow: Kolos, 1992. – 448 p.
3. Roginskiy, V. A. Kinetika okisleniya efirov polinenasyischennyih zhirnyih kislot, ingibirovannogo zameschennyimi fenolami [Text] / V. A. Roginskiy // Kinetika i kataliz. – 1990. – Vol. 31, Issue 3. – P. 546–552.
4. Demydov, I. M. Vplyv stupenya nenasychenosti oliy na sklad vtorynnykh produktiv yikh okysnenya [Text]: tez. dop. Mizhn. nauk.-tekhn. konf. / I. M. Demydov, A. V. Hryhorova // Tekhnichni nauky: stan, dosyahnennya i per-spektyvy rozvytku m»yasnoyi, oliye-zhyrovoyi ta molochnoyi haluzey, 2012. – P. 42–43.
5. Demidov, I. N. Opredelenie srokov hraneniya zhirov i zhirovyih produktov uskorennyim metodom [Text]: tez. dop. VII Mezhd. konf. / I. N. Demidov, D. V. Nevmivaka // Maslozhirovaya otrasl: tehnologii i ryinok, 2014. – P. 27–28.
6. Denysova, A. Yu. Doslidzhennya vplyvu zhyro-mahnetytovoyi suspenziyi na termin zberihannya tvarynnykh zhyriv [Text]: tez. dop. Mizhnar. nauk.-prakt. konf. / A. Yu. Denysova, Y. V. Tsykhanovskaya, O. B. Skorodumova, Ya. M. Honcharenko, H. O. Pryymak, I. V. Shevchenko // Prohresyvna tekhnika ta tekhnolohiyi kharchovykh vyrobnytstv, restorannoho ta hotel'noho hospodarstv i torhivli. Ekonomichna stratehiya i perspektyvy rozvytku sfery torhivli ta posluh. – 2013. – Part 1. – P. 71–72.
7. Ilyuha, N. G. Tehnologiya proizvodstva i pokazateli kachestva pischevoy dobavki na osnove magnetita [Text] / N. G. Ilyuha, Z. V. Barsova, V. A. Kovalenko, I. V. Tsihanovskaya // Eastern-European Journal of Enterprise Technologies. – 2010. – Vol. 6, Issue 10 (48). – P. 32–35. – Available at: http://journals.uran.ua/eejet/article/view/5847/5271
8. Tsihanovskaya, I. V. Izuchenie rastvorimosti magnetita v usloviyah, imitiruyuschih pischevaritelnyie protsessyi zheludochno-kishechnogo trakta [Text] / I. V. Tsihanovskaya, A. Yu. Denisova, O. B. Skorodumova, E. Ya. Levitin, V. A. Kovalenko, A. V. Aleksandrov, Z. V. Barsova // Eastern-European Journal of Enterprise Technologies. – 2012. – Vol. 6, Issue 6 (60). – P. 29–31. – Available at: http://journals.uran.ua/eejet/article/view/5547/4988
9. Tsykhanovs'ka, I. V. Doslidzhennya protsesiv okysnyuval'nykh ta termichnykh peretvorenn' v systemi: oliya – lipido – mahnetytova suspenziya [Text]: zb. nauk. pr. / I. V. Tsykhanovs'ka, Z. V. Barsova, I. M. Demydov, L. F. Pavlots'ka // Prohresyvna tekhnika ta tekhnolohiyi kharchovykh vyrobnytstv restorannoho hospodarstva i torhivli. – 2015. – Vol. 1 (21). – P. 353–362.
10. Krushenko, G. G. Problemyi opredeleniya razmerov nanochastits [Text] / G. G. Krushenko, S. N. Reshetnikova // Vestnik Sibirskogo gosudarstvennogo aerokosmicheskogo universiteta imeni akademika M. F. Reshetneva. – 2011. – Vol. 2. – P. 167–170.
11. Suzdalev, I. P. Nanotehnologiya: fiziko–himiya nanoklasterov, nanostruktur i nanomaterialov [Text] / I. P. Suzdalev. – Moscow: KomKniga, 2006. – 365 p.
12. Kecskes, L. J. Characterization of a nanosized iron powder by comparative methods [Text] / L. J. Kecskes, R. H. Woodman, S. F. Trevino, B. R. Klotz, S. G. Hirsch, B. L. Gersten // KONA. – 2003. – Vol. 21. – P. 143–149. doi: 10.14356/kona.2003017
13. NaBond Technologies Co [Electronic resource]. – Available at: http://www.nabond.com/TiN_nanopowder.html
14. Egorova, E. M. Stabilnyie nanochastitsyi serebra v vodnih dispersiyah, poluchennyih iz mitsellyarnyih rastvorov [Text] / E. M. Egorova et. al. // Zhurnal prikladnoy himii. – 2002. – Vol. 75, Issue 10. – P. 1620–1625.
15. Pimenova, N. V. Poroshki volframa, poluchennyie razlichnyimi sposobami [Text] / N. V. Pimenova // Tehnologiya metallov. – 2011. – Vol. 2. – P. 25–27.
16. Xu, R. Particle Characterization: Light Scattering Methods [Text] / R. Xu. – N.Y.: Kluwer Academic Publishers, 2001. – 410 p.
17. Mamani, J. B. Particokinetics: computational analysis of the superparamagnetic iron oxide nanoparticles deposition process [Text] / J. B. Mamani, T. T. Sibov, C. A. Caous, Jr. E. Amaro, L. F. Gamarra // International Journal of Nanomedicine. – 2012. – Vol. 2012:7. – P. 2699–2712. doi: 10.2147/ijn.s30074
18. Lou, W. On the Electromagnetic Scattering and Ab-sorption of Agglomerated Small Spherical Particles [Text] / W. Lou, T. T. Charalalampopoulos // Journal of Physics D: Applied Physics. – 1994. – Vol. 27, Issue 11. – P. 2258–2270. doi: 10.1088/0022-3727/27/11/004

19. Di Stasio, S. Feasibility of an Optical Experimental Method for the Sizing of Primary Spherules in Sub-Micron Agglomerates by Polarized Light Scattering [Text] / S. Di Stasio // Applied Physics B: Lasers and Optics. – 2000. – Vol. 70, Issue 4. – P. 635–643. doi: 10.1007/s003400050872
20. Mulholland, G. W. Measurement of 100 nm and 60 nm Particle Standards by Differential Mobility Analysis [Text] / G. W. Mulholland, M. K. Donnelly, Ch. R. Hadwood, S. R. Kukuck, V. A. Hackley, D. Y. H. Pui // Journal of Research of the National Institute of Standards and Technology. – 2006. – Vol. 111, Issue 4. – P. 257–312. doi: 10.6028/jres.111.022
21. Ivanov, L. A. Izmenenie svetovozvrascheniya ot steklyannyih mikrosharikov i progon kachestva sveto-vozvraschayuschih pokryitiy [Text] / L. A. Ivanov, D. V. Kizevetter, N. N. Kiselev et. al. // Opt. zhurn. – 2006. – Vol. 73, Issue 1. – P. 35–40.
22. Van de Hyulst, G. Rasseyanie sveta malyimi chastitsami [Text] / G. Van de Hyulst. – Moscow: IL, 1961. – 536 p.
23. Kerker, M. The scattering of light and other electromagnetic radiation [Text] / M. Kerker. – N.Y., London, Academic Press, 1969. – 666 p.
24. Xu, R. Particle Characterization: Light Scattering Methods [Text] / R. Xu. – N.Y.: Kluwer Academic Publishers, 2001. – 410 p.
25. Papok, I. M. Using the dynamic light-scattering method for the analysis of a blood-serum model solution [Text] / I. M. Papok, G. P. Petrova, K. A. Anenkova, E. A. Papish // Moscow University Physics Bulletin. – 2012. – Vol. 67, Issue 5. – P. 452–456. doi: 10.3103/s0027134912050104
26. Sohrabi-Gilani, N. Extraction of ultratrace amounts of nelfinavir from biological samples and pharmaceutical formulations using surfactant-modified magnetite nanoparticles followed by spectrophotometric determination [Text] / N. Sohrabi-Gilani, S. Makani // Microchemical Journal. – 2016. – Vol. 129. – P. 332–338. doi: 10.1016/j.microc.2016.06.003
27. Sutorikhin, I. Issledovaniya kontsentratsii i razmerov chastits vodnoy vzvesi s pomoschyu opticheskogo metoda fluktuatsiy prozrachnosti [Text] / Sutorikhin, I., Bukaty, V., Zalaeva, U., & Akulova, O. // Izvestiya of Altai State University. – 2013. – Vol. 1, Issue 2. – P. 189–193. doi 10.14258/izvasu(2013)1.2-39
28. Ershov, A. E. Effects of Size Polydispersity on the Extinction Spectra of Colloidal Nanoparticle Aggregates [Text] / A. E. Ershov, I. L. Isaev, P. N. Semina, V. A. Markel, S. V. Karpov // Physical Review B. – 2012. – Vol. 85, Issue 4. doi: 10.1103/physrevb.85.045421
29. Patent. na korisnu model # 54284, MPK S 01 G 49/00. SposIb otrimannya magnetitu [Text] / Ilyuha M. G, Tsihanovska I. V., Barsova Z. V., TImofeEva V. P., Vedernikova I. O. – published: 10.11.2010. Byul. # 21. – 4 p.
30. Van de Hulst, H. Light Scattering by Small Particles [Text] / H. Van de Hulst. – N.Y.: J. Willey & Sons, 1957. – 536 p.
31. Voyutskiy, S. S. Kurs kolloidnoy himii; 2-e izd. [Text] / S. S. Voyutskiy. – Mosocw: Himiya, 1975. – 512 p.
32. Ivanov, L. A. Izmenenie svetovozvrascheniya ot steklyannyih mikrosharikov i progon kachestva svetovozvraschayuschih pokritiy [Text] / L. A. Ivanov, D. V. Kizevetter, N. N. Kiselev et. al. // Opt. zhurn. – 2006. – Vol. 73, Issue 1. – P. 35–40.
33. Kizevetter, D. V. Odnovremennoe izmerenie razmerov i skorosti dvizheniya chastits [Text] / D. V. Kizevetter, V. I. Malyugin // Zhurn. tehn. fiziki. – 2009. – Vol. 79, Issue 2. – P. 90–95.
34. Chekhun, V. Mahnitni nanostruktury v pukhlynnykh klitynakh [Text] / V. Chekhun, S. Horobets', O. Horobets', I. Dem»yanenko // Visn. NAN Ukrayiny. – 2011. – Vol. 11. – P. 13–20.
35. Alexandrov, A. Stability and morphological characteristics of lipid-magnetite suspensions [Text] / A. Alexandrov, I. Tsykhanovska, T. Gontar, N. Kokodiy, N. Dotsenko // Eureka: Life Sciences. – 2016. – Vol. 3 (3). – P. 14–25. doi: 10.21303/2504-5695.2016.00143